ISSN: 0067-2904

The study of the Effect of Ionospheric Variables on the Astronomical Radio Signal

Muhanad H. Khudhur[1*], Monim H. Al-Jiboori[1], Kamal M. Abood[2]
[1]*Atmospheric Science Department, College of Science, Mustansiriyah University, Baghdad, Iraq*
[2]*Astronomy and Space Department, College of Science, University of Baghdad, Baghdad, Iraq*

Received: 7/2/2023 Accepted: 29/9/2023 Published: 30/11/2024

Abstract

In this work, the effect of the ionospheric variables on the astronomical radio signal was studied. Florida station, for the year 2014, was selected and the actual observation data of the Jupiter signal from the Radio JOVE Data Archive was used. The Radio Jove Pro software was used to determine the number of radio emissions from Jupiter that were supposed to occur. The data of the electron density and temperatures of the ionosphere for altitudes 200-500 kilometers were taken from the International Reference Ionosphere (IRI) site, where 116 supposed events were obtained, and after applying determinants for the angle of elevation of Jupiter and the elevation of the sun, this number was reduced to 45. This work aims to focus on the role of the ionosphere in blocking the radio signal coming from Jupiter. It was found that 28 events were actually observed, while 17 events were not observed. The possibility of observing is better after sunset and depends on Jupiter's height above the horizon relative to the observer. The value of F_2 peak density during the night time and along the year was about 10^{11} to 10^{12} m^{-3} and at a height of about 270-360 km. Approximately 82% of the observations occurred when the F_2 peak density was less than 6×10^{11} m^{-3} and the height was greater than 300 km, and approximately 82% of the cases of non-observation occurred when the F_2 peak density was greater than 6×10^{11} m^{-3} and the height was less than 300 km. The probability of observation is greatly affected by the relationship between the value of the electron density and its height.

Keywords: Ionosphere, Jupiter emission, astronomical radio signal.

دراسة تأثير متغيرات الأيونوسفير على الاشارة الراديوية الفلكية

مهند حسين خضر[1*], منعم حكيم خلف[1], كمال محمد عبود[2]
[1] قسم علوم الجو, كلية العلوم, الجامعة المستنصرية, بغداد, العراق.
[2] قسم الفلك والفضاء, كلية العلوم, جامعة بغداد, بغداد, العراق.

الخلاصة

في هذا العمل تم دراسة تاثير متغيرات الايونوسفير على الاشارة الراديوية الفلكية. اختيرت محطة فلوريدا لسنة 2014 وتم استخدام بيانات الرصد الفعلي لأشارة المشتري المتاحة في ارشيف (Radio JOVE Data Archive) و بيانات برنامج (Radio Jove Pro. Software) لتحديد عدد الانبعاثات الراديوية للمشتري المفترض حدوثها. بيانات الكثافة الالكترونية و درجات الحرارة للايونوسفير للارتفاعات 200−500 كم اخذت من موقع ((International Reference Ionosphere (IRI) , وتم الحصول على 116 حدث مفترض

*Email: muhanad.hussien2005@gmail.com

وبعد تطبيق محددات زاوية ارتفاع المشتري و ارتفاع الشمس تم تخفيض هذ العدد الى 45, يهدف العمل الى التركيز على دور الايونوسفير في حجب الاشارة الراديوية القادمة من المشتري. حيث وجد ان 28 حدث قد رصد فعليا و 17 حدث لم يتم رصده. ان امكانية رصد اشارة المشتري الراديوية تكون افضل بعد غروب الشمس وعندما يكون المشتري بارتفاع اعلى فوق الافق نسبة للراصد. ان اعلى قيمة للكثافة الالكترونية خلال الليل كانت (10^{12}–10^{11} m^{-3}) وبارتفاع 270–360 كم. 82% تقريبا من الحالات المرصودة حدثت عندما كانت اعلى قيمة للكثافة الالكترونية اقل من (6×10^{11} m^{-3}) وبارتفاع اعلى من 300 كم في حين 82% تقريبا من الحالات الغير مرصودة حدثت عندما كانت اعلى قيمة للكثافة الالكترونية اكبر من (6×10^{11} m^{-3}) وبارتفاع اقل من 300 كم. ان احتمالية الرصد تتأثر بشكل كبير بالعلاقة بين قيمة الكثافة الالكترونية و إرتفاعها.

1. Introduction

For radio astronomers, the short radio wave is the only way to get through the atmosphere and reach the ground. The radio window refers to the principal frequency bands that are able to penetrate the atmosphere and cover frequencies between 5 MHz and 30 GHz. The ionosphere's ability to reflect signals back into space limits the window's low-frequency end, while the atmosphere's ability to absorb radio waves determines its upper limit [1].

The ionosphere is the region of the Earth's atmosphere that extends roughly from 50 to 1000 kilometers above the Earth's surface [2]. Where the intensities of ultraviolet and X-ray solar radiation are sufficient to ionize atoms and molecules [3]. It is characterized by containing ionized particles and atoms and free electrons in addition to neutral air particles. It is formed as a result of the ionization of atoms and molecules due to short-wavelength solar radiation. The energy of these waves exceeds the bonding energy between the atom and its electrons, which leads to the separation of an electron from the atom or molecule to form a free electron and a positive ion. Repeating this process leads to the formation of this region, known as the ionosphere [4]. Although the ionosphere's structure is intricate and constantly changing, it may generally be split into three separate layers: D, E and F from lowest to highest. The D and E layers are located at a lower altitude, where the pressure is higher and the recombination rate for ions is very high at these pressures, so the D and E layers disappear very quickly after sunset, but the F layer is located at a lower pressure region where recombination is very slow. Recombination is the reverse process of ionization [5]. The D layer is found within the altitude range of 50-90 km, and the E layer is found at altitudes ranging from 90-150 km. For radio waves, the D layer serves as a refractive and absorptive medium [6]. From 150 to 500 km above the surface of the Earth, there is the highly ionized F layer [3]. The F layer is the most important layer for long-distance communications. During the daytime, the F layer is often divided into two sub-layers: F_1 which extends from 150 to 250 km, and F_2 which extends from 250 to 500 km [6]. The F layer's primary role is to reflect incoming terrestrial waves back to the Earth while also reflecting incoming extraterrestrial waves to prevent them from reaching the surface of the Earth [3]. There are daily, seasonal, and annual changes in the ionization of this layer, leading to variations in electron density and its height [7]. Most of the ionosphere becomes ionized throughout the day as a result of the sun's intense UV radiation [1].

The electronic production is at its largest at the local noon and in the summer, and increases with decreasing latitude, while the height of the layer is the least possible at the local noon and in the summer, and increases with the increase in latitude [8]. The electron density of the layer and the angle of solar incidence affect how intense the F layer is. This explains why, during a specific time each day when the layer was highly ionized, intense

man-made signals from all over the world were reflected onto our radio telescope, making it impossible to detect solar radiation [9].
Radio astronomical sources radiate at a variety of frequencies. Jupiter is one of these sources, emitting radio waves ranging in frequency from 10 kHz to 300 GHz. This emission is classified into several categories. The kilometric emission (10-1000 KHz) is the lowest, while hectometric (1-3 MHz), decametric (3-40 MHz), and decimetric (0.1-300 GHz) frequencies are also available [1]. Jovian emissions are typically not discernible during the day. Since Jovian emissions are less intense than solar emissions and more likely to be enveloped by noise, studies of the planet are typically conducted at night [9]. It is preferable to observe Jupiter's emissions in the absence of the sun when Jupiter is at a high peak position in the astronomical sky [10].

The range of the strongest radio emissions from Jupiter is roughly 50 KHz to 40 MHz. However, frequencies below about 15 MHz are not detectable at the Earth's surface because the Earth's ionosphere reflects them back into space. This is why we are interested in emission frequencies between 18 and 24 MHz, because it is much above the ionospheric cut-off frequency and it is not near manmade broadcast frequencies, where many observers tune in at 20.1 MHz. It has been discovered that the emissions depend on Jupiter's longitude and Jupiter's emissions are most likely to be found in the three longitude regions designated A, B, and C. Additionally, it has been discovered that certain orbital configurations of Jupiter's moon (Io) result in a significant increase in emissions. These improved emissions are Io-A, Io-B, and Io-C. Jupiter hides behind the sun for several months, making it invisible to radio telescopes. Several things influence our capacity to pick up Jupiter's emissions include: the state of the ionosphere of the Earth, the relative locations of the Earth and Jupiter in their orbits around the sun, and the location of Jupiter relative to our antenna (Jupiter must be above the horizon where the antenna is located). It is possible to predict when radio emissions are likely to occur, since the positions of Jupiter, the Earth and Jupiter's moon (Io) are well known [11].

2. Study Area

The location of the study was chosen depending on the availability of observational data for Jupiter's radio emissions. The study was carried out for the year 2014 and the geographic location of the AJ4CO Observatory, which is located in High Springs, Florida, USA at latitude 29.8369° N, longitude 82.6213° W. The elevation above sea level is about 16 m (see Figure 1). AJ4CO Observatory is operated by Dave Typinski, amateur radio call sign AJ4CO. The observatory's primary concern is radio astronomy in the 16-32 MHz region of the radio frequency spectrum, more or less the upper half of the HF band, with a focus on Jupiter's radio emissions in particular [12].

Figure 1: High Springs, AJ4CO Observatory [12] [13].

3. Data Sources

Two websites and one software program were used to gather data for this study, and they are described as follows:

3.1. Radio JOVE Data Archive

The observations made by an astronomy group using the radio Jove telescope at a frequency of 20.1 MHz for Jupiter and certain radio storm bursts are kept on the NASA website (http://radiojove.gsfc.NASA.gov). The data archive contains all observational data, including observer names, station locations (latitude and longitude), dates, times, and item storm types (see Figure 2). The archive of observations is available from 1999 to the present time. Unfortunately, monitoring data is not available continuously (only intermittently for years and stations). The data of the year 2014 from the Florida station was used. The selection of this station is based on the number of observations that are available in the data archive [14].

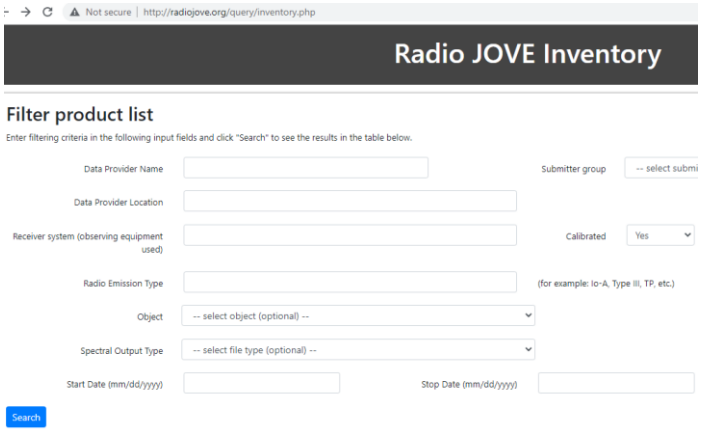

Figure 2: Radio JOVE Data Archive [14].

3.2. The International Reference Ionosphere

The International Reference Ionosphere (IRI) is a global model supported by the International Union of Radio Science (URSI) and the Committee on Space Research (COSPAR). In the late 1960s, these groups established a working group to develop an empirical standard model of the ionosphere based on all available data sources. The model has been released in a number of iterations that have gradually improved. IRI offers monthly averages of the electron density, electron temperature, ion temperature, and ion composition in the ionosphere between the altitudes of 60 and 2000 km, for a specified place, time, and date (see Figure 3). New models and ionosphere-related data are frequently added to the IRI [15].

Information is gathered from ionosondes, incoherent scatter radars, topside sounder satellites, GPS, and rocket observations. In some situations and at particular times, the IRI model is less accurate. The F layer of the ionosphere, for instance, is very well predicted by the IRI since it primarily uses GPS and ionosonde data; however, the D and E layers, which have lower electron densities, are not well detected using GPS or ionosonde data. This indicates that the D and E layer models are less accurate because they are based on less data than the F layer model [16].

Figure 3: International Reference Ionosphere [15].

3.3. The Radio Jove Pro. Software

This program has certain features that are helpful in forecasting storms on the sun and Jupiter, planning observations, and following the motions of Jupiter and its moon, Io. It was made to be used by astronomers utilizing the Radio JOVE telescope (see Figure 4). These features were used in this study to determine how many Jupiter storm observations must be made during 2014, particularly at the Florida, USA station [17].

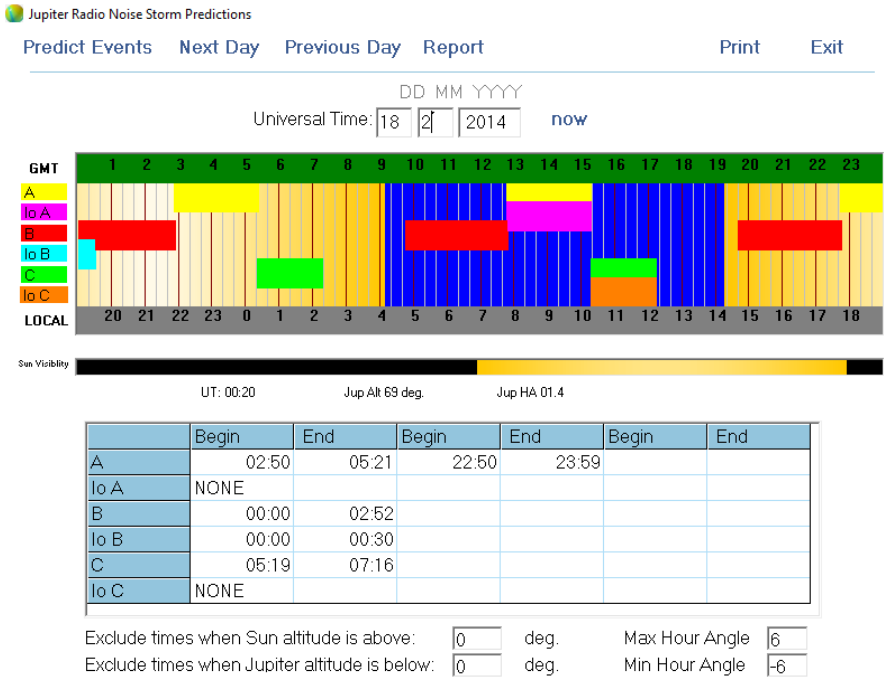

Figure 4: The Radio Jove Pro. Software [18].

4. Results and Discussion

For the year 2014, and by using the Radio JOVE Pro software based on the movement of Jupiter and its satellite Io, there are about 116 events that refer to the likelihood that an observer would be able to detect a Jupiter radio storm using the Radio JOVE telescope.
Due to the sun's higher radio emission density compared to Jupiter's, the likelihood of observing a Jupiter storm burst is minimal because when the sun and Jupiter are both visible above the Earth's horizon at the same time, it is usually necessary to observe Jovian emissions well after dusk and before dawn.

The height of the F_2 peak (hmF_2) and the density of the F_2 peak (NmF_2) data were taken from IRI for the year 2014 and for the study site, using the OriginLab2021 program, NmF_2 and hmF_2 were plotted for the times 00:00, 06:00 and 12:00 UTC which represented the night period along the year. Figure 5 shows that hmF_2 ranges between approximately 270 and 360 km during the night, and the NmF_2 ranges between 10^{11} and 10^{12} m^{-3}. It is noted that the highest NmF_2 (at night) is at 00:00 UTC in the spring, and the lowest NmF_2 is at 06:00 UTC in the winter.

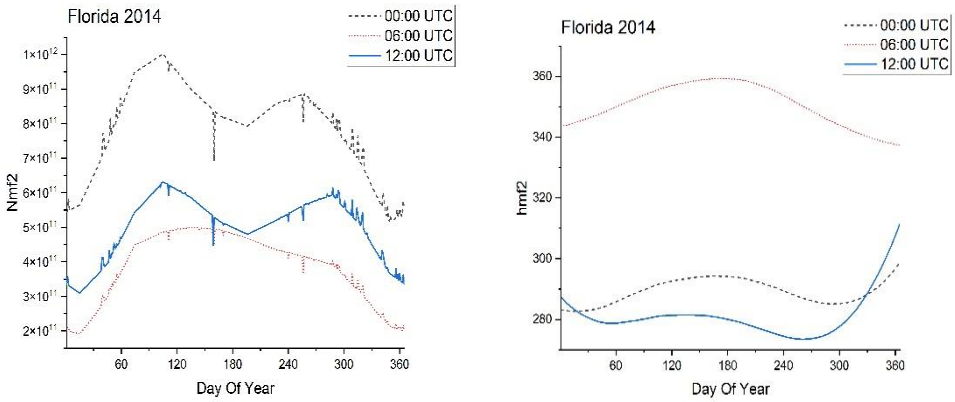

Figure 5: Represents NmF_2 and hmF_2 during the night throughout the year 2014, local time =UTC-5

It is noted that hmF_2 is inversely proportional to NmF_2, so the highest hmF_2 is accompanied by the lowest value of NmF_2 at 06:00 UTC, and the lowest hmF_2 is at 00:00 UTC and 12:00 UTC-near sunrise and sunset and accompanies the highest value of NmF_2 .
From the Radio JOVE Pro software, the height of Jupiter above the horizon according to the Florida location was obtained. The number of the likelihood of observations was reduced to be just 45 events due to the sun's visibility.

The predicted unobserved events (UN-OBS) were taken from the Radio JOVE Pro software while the actual observations (OBS) were taken from Radio JOVE data archive for the Florida station, which were tabulated according to date, time, altitude of Jupiter and the sun and type of satellite Io storm (see Table 1). From this table the predicted unobserved events are only 17 and the actual observations are only 28.

Table 1: The dates of 17 predicted unobserved events (UN-OBS) and 28 actual observations (OBS) for Florida station of the year 2014.

OBS Date	UN-OBS Date	UTC	Jupiter altitude angle	Sun altitude angle	Storm type
05/01/2014		06:53	71.85	-69.7	Io-A
16/01/2014		03:24	69.7	-59.9	Io-A
17/01/2014		04:36	82.6	-74.2	Io-B
23/01/2014		04:13	83.04	-68.9	Io-A/C
24/01/2014		04:20	83	-70.3	Io-B
30/01/2014		03:40	83.08	-61.18	Io-A/C
31/01/2014		05:03	70.81	-75.81	Io-B
06/02/2014		03:02	82.6	-52.03	Io-A/C
13/02/2014		03:44	75.41	-59.47	Io-A
	18/02/2014	00:30	63.31	-17.3	IO-B
	23/02/2014	23:59	61.8	-9.5	IO-A
	24/02/2014	00:57	74	-22	IO-A/C
25/02/2014		01:56	83.45	-34.93	Io-B
	02/03/2014	23:59	68	-8.5	IO-A
03/03/2014		01:30	83.45	-28.44	Io-C
04/03/2014		01:16	82.91	-25.26	Io-B
	09/03/2014	23:59	73.7	-7.5	IO-A
10/03/2014		01:04	83.48	-21.8	Io-C
11/03/2014		02:22	70.62	-38.16	Io-B
	17/03/2014	00:36	83.46	-14.76	IO-A/C
	19/03/2014	01:38	73.44	-27.71	IO-A
	24/03/2014	01:45	68	-28	IO-A
04/04/2014		23:57	80.6	-3.99	Io-B
	05/04/2014	00:00	80.27	-4.42	IO-B
	10/04/2014	23:57	76.77	-3.2	IO-C
11/04/2014		23:57	76.09	-3.07	Io-B
	12/04/2014	00:00	75.69	-3.5	IO-B
	18/04/2014	00:06	70.18	-3.98	IO-C
26/04/2014		23:57	65.39	-1.09	Io-A
	27/04/2014	00:00	64.9	-1.51	IO-A
	03/05/2014	23:57	60.3	-0.17	IO-A
18/10/2014		11:22	62.38	-1.6	Io-B
	26/10/2014	10:54	62.01	-8.74	IO-A
02/11/2014		11:33	72.54	-1.69	Io-A
09/11/2014		11:39	75.09	-1.55	Io-A
16/11/2014		11:34	75.02	-3.52	Io-A
	23/11/2014	11:32	73.22	-5.07	IO-A
	26/11/2014	09:02	61.26	-37.34	IO-B
05/12/2014		08:48	65.07	-41.62	Io-B
11/12/2014		08:46	68.8	-42.85	Io-A/C
12/12/2014		09:48	74.97	-29.62	Io-B
18/12/2014		09:28	74.98	-34.66	Io-A/C
19/12/2014		09:44	73.94	-31.35	Io-B
25/12/2014		08:48	75.07	-44.08	Io-A/C
26/12/2014		10:33	62	-21.9	Io-B

Using the OriginLab2021 program, the relationship between the ionospheric variables and height was plotted for the time of occurrence of Jupiter's emissions for the 28 observed and 17 predicted unobserved events. However, four samples have been selected to display here in Figure 6.

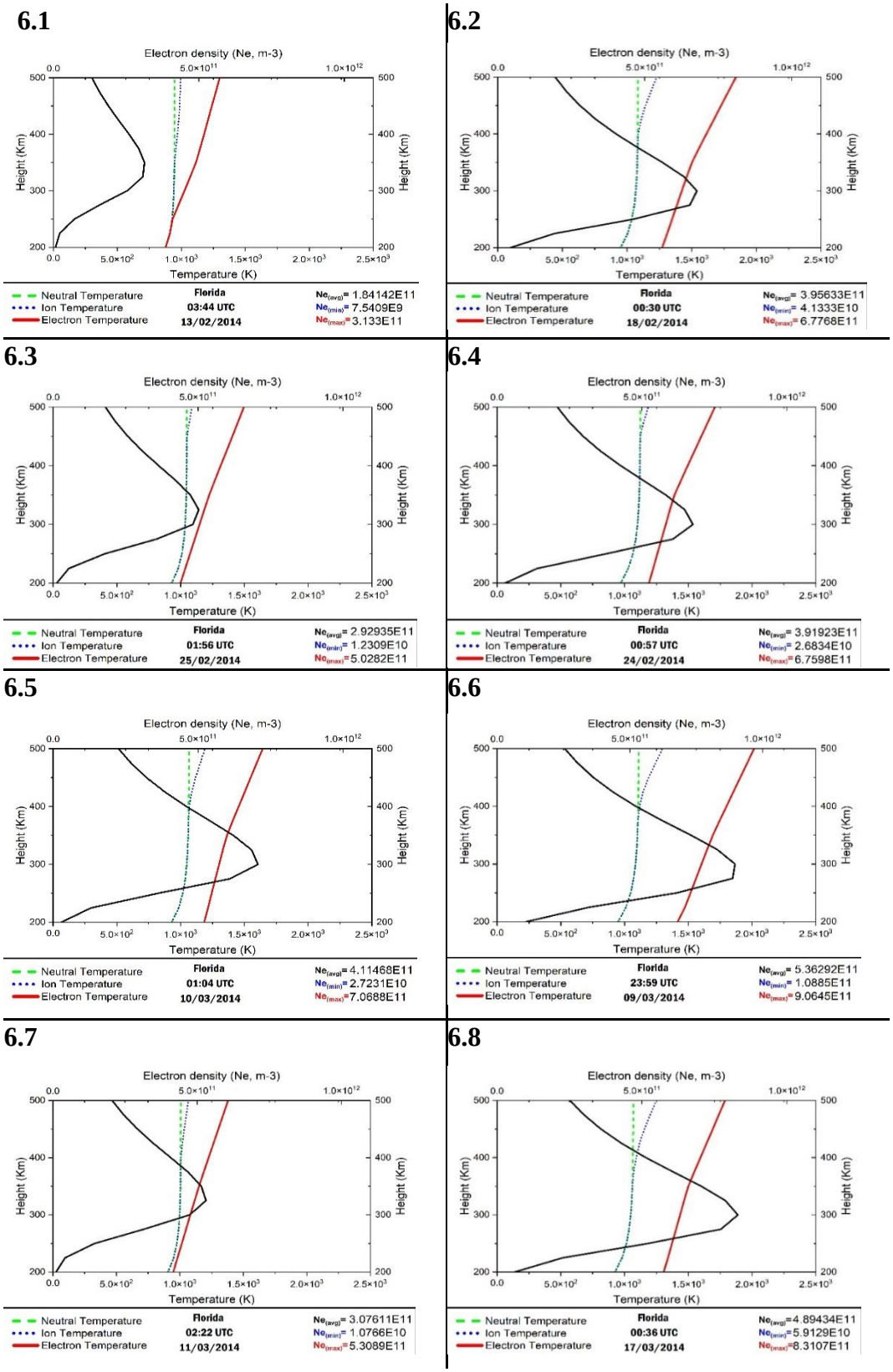

Figure 6: The vertical change of ionospheric variables (electron density, neutral temperature, ion temperature, and electron temperature with height). The black curve represents the electron density and the three colored curves represent the temperatures. Figures 6.1, 6.3, 6.5 and 6.7 for observed cases and 6.2, 6.4, 6.6, 6.8 for predicted unobserved cases, local time =UTC-5.

Figure 6 shows the vertical change of the electron density, neutral temperature, ion temperature, and electron temperature with height. It became clear that the electron density increases with height up to the height of the F_2 peak and then started decreasing. As for the cases that were observed, the F_2 layer had a lower electron density and a higher height, while in the unobserved cases, the vertical change with the height of the electron density was sharper with a lower height of the F_2 peak. As for the temperatures, it was noted that the vertical change of neutral temperature and ion temperature was very slight, but the change of electron temperature with height increased sharply in cases that were unobserved.

The data of the height of the F_2 peak (hmF_2) and the density of the F_2 peak (NmF_2) for 17 predicted unobserved events (UN-OBS) and 28 actual observations (OBS) were taken from IRI, shown in Table 2.

Table 2: The height of the F_2 peak (hmF_2) and the density of the F_2 peak (NmF_2) for 17 predicted-unobserved events (UN-OBS) and 28 actual observations (OBS) for Florida station of the year 2014

OBS Date	UN-OBS Date	Height of F_2 peak	Density of F_2 peak
dd/mm/yy	dd/mm/yy	hmF2(km)	NmF2(m^{-3})
05/01/2014		342.8	2.16E+11
16/01/2014		331.9	2.34E+11
17/01/2014		341.5	2.01E+11
23/01/2014		340.2	2.28E+11
24/01/2014		341.2	2.29E+11
30/01/2014		337.2	2.69E+11
31/01/2014		345.3	2.43E+11
06/02/2014		331.8	3.22E+11
13/02/2014		340.2	3.15E+11
	18/02/2014	290.7	6.82E+11
	23/02/2014	284.8	8.49E+11
	24/02/2014	299.1	6.76E+11
25/02/2014		317.9	5.05E+11
	02/03/2014	285.8	8.55E+11
03/03/2014		310.5	5.95E+11
04/03/2014		305.9	6.38E+11
	09/03/2014	286.8	9.06E+11
10/03/2014		302.7	7.07E+11
11/03/2014		327.3	5.31E+11
	17/03/2014	295.3	8.32E+11
	19/03/2014	315	6.57E+11
	24/03/2014	317.9	6.57E+11
04/04/2014		289.9	9.91E+11
	05/04/2014	290.4	9.84E+11
	10/04/2014	290.6	1.00E+12
11/04/2014		290.7	1.00E+12
	12/04/2014	291.2	9.97E+11
	18/04/2014	292.5	9.77E+11
26/04/2014		292	9.70E+11
	27/04/2014	292.4	9.60E+11

	03/05/2014	292.7	9.42E+11
18/10/2014		296.3	4.20E+11
	26/10/2014	311.4	3.20E+11
02/11/2014		293.6	4.25E+11
09/11/2014		292.5	4.30E+11
16/11/2014		297.6	4.26E+11
	23/11/2014	301	3.57E+11
	26/11/2014	330.8	2.34E+11
05/12/2014		326.7	2.28E+11
11/12/2014		323.7	2.19E+11
12/12/2014		325.3	1.77E+11
18/12/2014		322.2	1.78E+11
19/12/2014		322.9	1.69E+11
25/12/2014		316	2.03E+11
26/12/2014		323.9	1.77E+11

The data in Table 2, represented by a histogram, (see Figure 7) displays the frequency of NmF_2 and hmF_2 for both observed and unobserved cases.

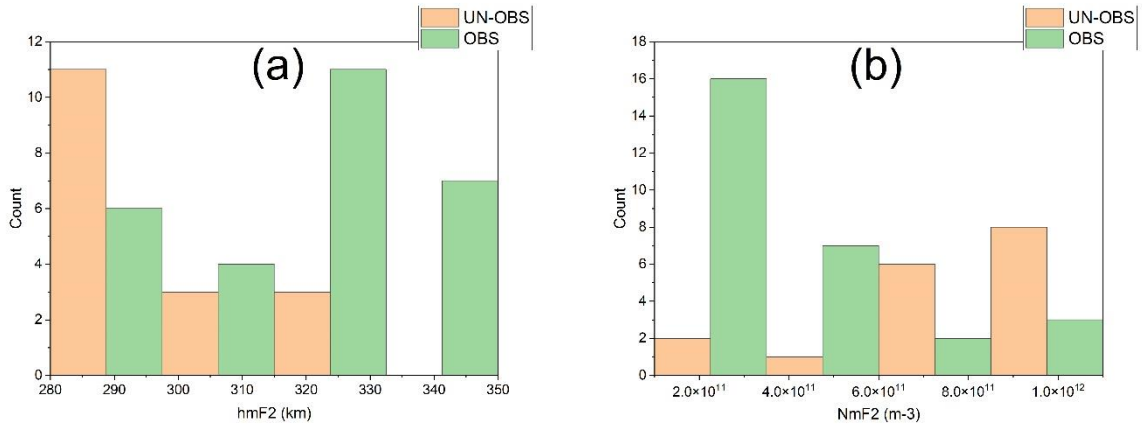

Figure 7: Histograms for both of observed(OBS) and unobserved(UN-OBS) cases (a)shows the height of the F_2 peak (hmF_2) and (b) shows the F_2 peak density(NmF_2).

From Table 2 and Figure 7, it was noted that:
For the observed cases, the highest recurrence was for hmF_2 greater than 300 km and NmF_2 less than 6×10^{11} m^{-3}, while the highest recurrence for the predicted unobserved cases was for hmF_2 less than 300 km and NmF_2 greater than 6×10^{11} m^{-3}.
The data were analyzed and classified according to the density of the F_2 peak (NmF_2) and the height of the F_2 peak (hmF_2) and the results were displayed in the form of percentages representing the probability of observation (see Table 3).

Table 3: The probability of observation, expressed as a percentage, has been categorized based on the height of the F_2 peak (hmF_2) and the density of the F_2 peak (NmF_2) for 17 predicted unobserved events and 28 actual observations at the Florida station in the year 2014.

	Cases number	NmF_2 (m^{-3})	hmF_2 (km)	Percentage %
28 observed cases	5	$6.38\times10^{11} - 1.00\times10^{12}$	290-327	17.86
	23	**1.69×10^{11} - 5.95×10^{11}**	**292.5-345.3**	**82.14**
17 predicted unobserved cases	3	2.34×10^{11} - 3.57×10^{11}	301-330.8	17.65
	14	**$6.57\times10^{11} - 1.00\times10^{12}$**	**284.8-317.9**	**82.35**

The 23 observed cases mentioned in the above table included 19 cases (82.61%) with hmF_2 310.5-345.3 km and the 14 predicted unobserved cases included 12 cases (85.71%) with hmF_2 284.8-299.1 km.
Approximately, 82% of the observations occurred when the F_2 peak density (NmF_2) was less than 6×10^{11} m^{-3} and the height was greater than 300 km, while approximately 82% of the cases of non-observation occurred when the F_2 peak density(NmF_2) was greater than 6×10^{11} m^{-3} and the height was less than 300 km.

5. Conclusion

The possibility of observing Jupiter's radio emissions after sunset depends on Jupiter's height above the horizon relative to the observer.
The value of the F_2 peak density (NmF_2) ranges between 10^{11} and 10^{12} m^{-3} during the night and at a height of 270-360 km.

The probability of observation was greatly affected by the relationship between the value of the electron density and its height.

The observation probability increases when the electron density is low and at a high altitude, while it decreases when the electron density is higher and at a lower altitude.
In order to get rid of the effect of the ionosphere on the observation of Jupiter's radio signal, the observation instrument must be at an altitude exceeding 300 km.

References

[1] J. Thieman, C. Higgins and L. Garcia, "The Effects of Earth's Upper Atmosphere on Radio Signals," [Online]. Available: https://radiojove.gsfc.nasa.gov/education/lesson_plans /complete .pdf. [Accessed Feb. 11, 2023].

[2] A. A. Temur and A. F. Ahmed, "Plasma Characteristics of the Earth's Ionosphere in F-layer," *Iraqi Journal of Science*, vol. 63, no. 7, pp. 3225-3235, 2022.

[3] M. C. Kelley, *The earth Ionosphere: Plasma Physics and Electrodynamics*, 2nd ed., san diego: Academic Press, 2009, pp. 1-6.

[4] M. H. Ahmed, "Estimation of electrical conductivity of the ionospheric layer over Baghdad," M.S. thesis, Dept. Atmospheric Sciences, Univ. Al-Mustansiriyah, Baghdad, Iraq, 2008.

[5] M. M. S. Al-gubory, "Investigating the Validity of the IRI Model for the Total Electron Content During Strong, Sever and Great Geomagnetic Storms," M.S. thesis, Dept. Astronomy and Space, Univ. Baghdad, Baghdad, Iraq, 2015.

[6] A. A. Temur, A. F. Ahmed and R. A. Ali, "Determination of the Mathematical Model for Plasma Electronic," *Iraqi Journal of Science*, vol. 64, no. 3, pp. 1508-1517, 2023.

[7] A. A. Al-Shallal and N. M. Al-Ubaidi, "Comparing Ionospheric MUF using IRI16 Model with Mid-Latitude Ionosonde Observations and Associated with Strong Geomagnetic Storms," *Iraqi Journal of Science*, vol. 61, no. 12, pp. 3434-3445, 2020.

[8] A. D. al-Jubouri, "The phenomenon of the F layer spread in the ionosphere over the city of Baghdad," M.S. thesis, Dept. Atmospheric Sciences, Univ. Al-Mustansiriyah, Baghdad, Iraq, 2002.

[9] N. M. Ebadi and K. M. Abood, "Study of Sunspot Effect on Radio Jove Telescope Observation," *Iraqi Journal of Science*, vol. 55, no. 1, pp. 258-267, 2014.

[10] H. U. Alaa-AlDeen and K. M. Abood, "Study of Actual Jupiter Observation Days at UFRO Station During 2004 Year," *Iraqi Journal of Science*, vol. 57, no. 1c, pp. 768-774, 2016.

[11] W. D. Reeve, "Listening to Jupiter's Radio Storms Part 1," *Journal of radio user*, vol. 1, no. 1, pp. 32-37, 2009.

[12] D. Typinski, "AJ4CO Observatory," aj4co.org, [Online]. Available:

https://www.aj4co.org/index.html. [Accessed Feb. 29, 2023].

[13] "GPS Coordinates and Maps," gps-coordinates.net, [Online]. Available: https://www.gps-coordinates.net. [Accessed Jan. 20, 2023].

[14] "Radio JOVE Data Archive," Radio JOVE Project, [Online]. Available: https://radiojove.net/query/inventory.php. [Accessed Jan. 18, 2023].

[15] "International Reference Ionosphere - IRI (2016) with IGRF-13 coefficients," Community Coordinated Modeling Center, [Online]. Available: https://ccmc.gsfc.nasa.gov/modelweb/models/iri2016_vitmo.php. [Accessed Dec. 25, 2022].

[16] D. Bilitza, L.-A. McKinnell, B. Reinisch and T. Fuller-Rowell, "The international reference ionosphere today and in the future," *Journal of Geodesy*, vol. 85, no. 12, pp. 909-920, 2011.

[17] R. S. Flagg, *Listening to Jupiter: A Guide for the Amateur Radio Astronomer*, 2nd ed., Louisville, Kentucky: Radio-Sky Publishing, 2000, pp. 28-29.

[18] *Radio-Jupiter Pro 3*. (2001). Radio Sky Publishing. Accessed: Nov. 15, 2022, [Online]. Available: https://radiosky.com/rjpro3ishere.html.